

Enhancing the Thermal Stability of Polyamide 6 in Powder Bed Fusion via Primary and Secondary Antioxidant Incorporation

A. Jaksch^{1,2}, C. Cholewa^{1,2} and D. Drummer^{1,2}

¹Collaborative Research Center - Additive Manufacturing (CRC 814), Friedrich-Alexander-Universität
Erlangen-Nürnberg, Am Weichselgarten 10, 91058 Erlangen, Germany

²Friedrich-Alexander-Universität Erlangen-Nürnberg, Institute of Polymer Technology, Am Weichselgarten
10, 91058 Erlangen, Germany

Abstract

Polyamide 6 (PA6) is a thermoplastic material widely used in manufacturing for its excellent mechanical properties, such as high strength, stiffness, and toughness. However, its suitability for powder bed fusion (PBF) is limited due to its susceptibility to thermo-oxidative aging, resulting in material degradation and mechanical property deterioration over time. To address this issue, the efficacy of antioxidants in increasing the aging resistance of PA6 in PBF was investigated. Process-adapted analysis was employed using a coupled rheometer FTIR instrument to elucidate physical and chemical changes in the material. In addition, the viscosity number of the virgin and processed powder, the yellow index, and the part performance were evaluated. Results revealed that the addition of primary and secondary antioxidants significantly enhanced the aging resistance of PA6 in PBF, thereby increasing its potential as a suitable material for additive manufacturing applications.

Introduction

Powder bed fusion of polymers (PBF-LB/P) is an additive manufacturing process that uses a laser to selectively melt a powder material. It creates prototypes and functional parts with complex geometries and high accuracy. A thin layer of powder material is spread out, and a laser traces the desired part shape on the powder bed, melting the powder in that area. The platform is lowered, and another layer of powder is added. This layer-by-layer process is repeated until the parts are built. [1]

Variety of materials are commonly utilized in PBF-LB/P, with polyamide 12 (PA 12) being the most extensively employed material to date. Despite polyamides holding a significant market share in traditional manufacturing processes, PA 12 has a relatively minor role and is primarily used in special applications. The more commonly used polyamides, such as Polyamide 6 (PA 6) and Polyamide 6.6 (PA 6.6), are rarely utilized in PBF-LB/P. Although commercial PA 6 powders are available, challenges persist regarding the mechanical performance and aging behavior of the material. [2]

Typically, process temperatures in PBF-LB/P fall within the range of 170-300°C. These temperatures are determined by the melting and crystallization points of the polymer. The processing window is defined as the temperature gap between these points. Although the process chamber is filled with an inert gas atmosphere, a residual oxygen content remains. The level of this residual oxygen varies depending on the specific machine. As a consequence of the high temperature, extended process duration, and remaining oxygen, aging effects manifest in the powder material. This leads to reduced reusability and potential alterations in part properties. [1]

Stabilizers can be employed to mitigate the aging effects of polymers during processing and application. Typically, these stabilizers are customized for traditional processes characterized by short processing times and high temperatures, or for parts subjected to low temperatures and extended aging periods [3]. Unfortunately, for boundary conditions in PBF-LB/P, there is little to no knowledge of the behavior of traditional polymer stabilization. Therefore this work will focus on the aging behavior of PA 6 powder, and the stabilization of the material regarding thermo-oxidation effects.

Aging effects in polymers can generally be classified into two categories: physical aging and chemical aging. Physical aging occurs when the polymer molecules undergo rearrangements and changes in their physical structure due to external factors such as temperature, humidity, and stress. These effects are reversible after the melting of the polymer. Chemical aging occurs when the polymer molecules react with external agents, such as oxygen, UV light, and other chemicals. These reactions can lead to changes in the chemical structure of the

polymer, resulting in changes in its properties, such as color, solubility, and strength. Chemical aging is non-reversible due to changes in the polymer chain. [4]

Several chemical aging mechanisms can contribute to changes in polymers. These include thermal degradation, post-condensation, UV degradation, hydrolysis, oxidation, or a combination of these factors. Thermo-oxidation, for instance, can pose significant challenges in specific polymer applications. This is particularly true for applications involving high temperatures or prolonged exposure to oxygen. Autooxidation is another process that occurs in polymers upon exposure to oxygen. It results in the formation of free radicals, which can cause chain scission and other forms of degradation. The autooxidation cycle is a series of reactions that can occur in polymers during this process. This cycle is divided into three main stages: [3]

Initiation: This represents the initial stage of the cycle, where oxygen molecules interact with the polymer and generate free radicals. Various factors such as heat, UV radiation, and the presence of specific catalysts can trigger this process.

Propagation: During this stage, the free radicals formed in the initiation phase react with oxygen to produce new free radicals. These new radicals then further react with other polymer molecules, initiating a chain reaction that can result in polymer degradation, branching, or chain-entanglement.

Termination: The final stage of the cycle involves the reaction of free radicals with one another, forming stable products. This termination step brings an end to the chain reaction.

In PBF-LB/P studies mainly focus on the chemical aging by means of post-condensation of end groups unregulated polyamides such as PA12 [5] or PA11. During the process, chemical aging occurs in the PA 12 powder. In other studies, this material change is attributed to post-condensation in the solid phase [6]. The chain ends of the PA 12 macromolecules can react with each other, releasing water [7]. This results in an increase in molecular weight [6,8], and a corresponding increase in the melt viscosity of the material [9]. Changes in the average molecular weight are characterized, for example, using the viscosity number (VZ) or the melt volume flow rate (MVR) [6,10].

In addition to chemical aging, physical aging of the macroscopic particle morphology occurs at the particle level. Due to the tribo-mechanical stress during powder application and the accompanying thermal stress during the recoating process, the flowability of the powder decreases [6]. This decrease in powder flowability has been attributed to the smoothing of the particle surface, and a change in the concentration of flow aids on the particle surface [6]. This results in a decrease in the distance between the individual particles and an increase in the adhesion forces. However, no change in the particle size distribution was observed [6,10].

Further, there is a lot of work on thermo-oxidative aging and stabilizers, often with the focus on component properties after certain time intervals. Octavie et al. [11] investigated the aging for PA 11 for injection moulding. Regarding the impact of temperature during tensile testing, it has been noted that higher temperatures can delay the process of embrittlement. In other words, the decrease in strain at break occurs at higher oxidation conversion degrees. The origin of the transition from ductile to brittle is well known within a certain range of molecular weights [12], and allows the definition of a critical molar mass (M'_c). When the average molar mass (M_n) exceeds the M'_c , the sample exhibits ductile behavior. Other investigations have been carried out regarding the thermal oxidative aging of different polyamide variants. One such example involves the use of FT-IR spectroscopy by researchers to analyze the chemical and physical transformations that take place in PA 6 and PA 6.6 due to thermal degradation. The IR spectra obtained from these studies demonstrates comparable modifications in both PA 6 and PA 6.6, including the creation of carbonyl groups as a consequence of oxidation processes [13].

To facilitate the design of materials for the PBF-LB/P process, a comprehensive understanding of polymer aging mechanisms is crucial. While it is not possible to stabilize a polymer against thermal degradation, here are several strategies to mitigate the effects of oxidation. These include the use of antioxidants, stabilizers, and minimizing the polymer's exposure to oxygen and other degradation sources [3].

Stabilizers are substances incorporated into polymers to protect them from degradation caused by factors like heat, UV radiation, and oxygen. Various types of stabilizers are employed to safeguard polyamides from degradation, including antioxidants, UV absorbers, heat stabilizers, and processing stabilizers. Antioxidants are classified into primary and secondary antioxidants [3].

Primary antioxidants function by reacting with oxygen-containing polymer radicals formed during autooxidation. These highly reactive radicals are converted into inactive or less reactive compounds, effectively interrupting the radical chain reaction. Consequently, the antioxidants are consumed in this process [3].

Secondary antioxidants, on the other hand, are capable of reacting with hydroperoxides and decomposing them into non-radical products. By working in tandem with primary antioxidants, secondary antioxidants prolong the life span of primary antioxidants by decomposing hydroperoxides into non-radical compounds, thus impeding the formation of new radicals. The complementary actions of different types of stabilizers provide enhanced protection against excessive consumption [3].

Materials and Methodology

Material and machine

The experimental investigations employed a PA 6 material known as Ultramid B27 E, manufactured by BASF in Germany. This specific grade of Ultramid B27 E possesses a low viscosity, rendering it highly suitable for compounding and the production of monofilaments. Three stabilizers were used to increase the aging resistance: Two primary and one secondary antioxidant.

Sterically hindered phenolic antioxidant

Phenolic antioxidants are radical scavengers that prevent thermal degradation of many organic materials, such as polymers [14]. Their effectiveness increases when used in combination with phosphites, thioethers, and light stabilizers. Polymer radicals that are generated are effectively quenched through hydrogenation by the hydroxyl group. Therefore, phenolic antioxidants act as primary antioxidants.

Organophosphate

Organophosphate antioxidants are widely used additives in polymers to protect against oxidative degradation. They function by intercepting and neutralizing free radicals that initiate and propagate the oxidation process [15]. They act as secondary antioxidants, and efficiently convert hydroperoxides into non-radical products through their function as oxygen-scavenging phosphites. The usage of organophosphate antioxidants in combination with phenolic antioxidants can result in synergistic effects.

The materials were dried according to the manufacturer's recommendation and compounded into the PA 6 matrix using a twin-screw extruder MIC 27GL/44D from Leistritz GmbH, according to Table 1. Finally, the manufactured granulate was milled cryogenically to a powder material. The powder was dry blended with 0.1 wt.-% hydrophobic silica and 0.1 wt.-% pyrogenic alumina to improve the powder flowability.

Table 1: Compound recipes and additive concentration in wt.-%

	Reference (Ref.)	Compound 1 (D1)	Compound 2 (D2)
organophosphate	0 %	0.3 %	0.3 %
sterically hindered phenolic antioxidant – Type A	0 %	0.1 %	0.0 %
sterically hindered phenolic antioxidant – Type B	0 %	0 %	0.1 %

The experimental procedures were conducted utilizing a custom build laser sintering system capable of flexibly customizing all processing parameters. This system incorporates eight quartz radiator arrays, each independently controlled to ensure a homogeneous temperature distribution across the surface of the powder bed. A CO₂ laser, possessing a maximum nominal power of 50 W and a spot diameter of 500 μm, was employed to selectively melt the powder material. To minimize powder consumption, a downsized build chamber with dimensions of 100 x 100 mm² was utilized. Following a duration of one hour, the machine successfully achieved a residual oxygen content of approximately 1.5% measured inside the process chamber with an oxygen meter.

Prior to the processing stage, the powder underwent a drying process for a duration of four hours at a temperature of 70 °C in a vacuum atmosphere. The build procedure consisted of two layers, from which tensile bars were manufactured following the specifications outlined in [16]. A total of four tensile bars in xy-orientation were produced in each layer, employing an energy density of 0.06 J/mm². To achieve the desired energy density, a laser power of 18.7 W, a scan speed of 1250 mm/s, and a hatch distance of 0.25 mm were employed.

The build chamber temperature was set at 210 °C, while the removal chamber temperature was maintained at 150 °C. Each layer had a thickness of 120 μm, resulting in a layer time of 30 seconds. Prior to the start of the build

process, the machine was pre-heated for two hours, initially having a powder height of 5 mm. During this pre-heating period, an additional 5 mm of powder was added. The total build time amounted to 1.5 hours, after which the job was cooled for a duration of four hours within the machine.

Analysis Methods

Particle size distribution

The powder particle size distribution (PSD) was determined by image analysis using a QICPIC (Sympatec GMBH). In total 1,000,000 particles were used to calculate the PSD.

Compression depth

The powder compressibility was measured using the DHR 2 rotational rheometer from TA Instruments [11]. The measurements were conducted using a setup consisting of 25 mm parallel plates. The bottom plate was modified with a ring of an inner diameter of 27 mm to contain the powder material. To ensure consistency, a normal force of 0.2 N was applied to the sample before it was compressed at a constant rate by decreasing the gap height of the rheometer. The normal force was analyzed during the process. The measurements were repeated ten times.

DSC-Measurements

Dynamic and isothermal measurements were performed with the virgin powder by differential scanning calorimetry (Discovery 2500, TA-Instruments) under a dry N₂ atmosphere to characterize the melting and crystallization behavior of the powders. For the dynamic measurements, (2.5 ± 0.1) mg samples were heated and cooled twice from 0 °C to 260 °C with a 10 K/min ramp. For isothermal measurements, samples weighing (2.5 ± 0.1) mg were heated to 250 °C with a 60 K/min ramp and held for one minute. Subsequently, the samples were cooled down to a temperature of 200 °C at a rate of 60 K/min and kept isothermal for two hours.

Rheology + FTIR

In this study a combined measurement instrument called the rheonaut, manufactured by Thermo Electron GmbH in Germany, to measure the time depending aging effects simultaneously is used. The rheonaut integrates two techniques: Fourier-transform infrared spectroscopy (FTIR) and a rheometer as presented in [17,18]. FTIR was employed to evaluate changes in the polymer chain. This technique involves directing an infrared beam through an attenuated total reflectance (ATR) crystal into the sample, which is then analyzed using a deuterated triglycine sulfate (DTGS) detector. The FTIR measurements were performed using a Thermo Fisher Scientific Nicolet IS10 instrument; absorption measurements were recorded with a spectral resolution of 4 cm⁻¹ and 16 repeat scans. A spectral image was recorded every minute throughout the measurement. Simultaneously, the material's rheological properties were measured using a rheometer, specifically the HAAKE MARS 60 model. The rheological measurements were carried out with the following parameters: a frequency sweep with an angular frequency ranging from 0.1 rad/s to 628 rad/s was performed every 5 minutes. The gap between the parallel plates was set at 1 mm, and the temperature was set at 230 °C. A strain of 1% was applied during the measurements, and the experiments were conducted in ambient air. The rheometer utilized a 25 mm parallel plate measurement setup, with the ATR crystal positioned on the boundary area of the 25 mm plate, still covered with polymer. The measurement was carried out for three hours for each sample.

Viscosity number

The viscosity number (VN) is determined to characterize the changes in the viscosity and thus average molecular weight due to aging. The VN is measured according to DIN EN ISO 307. Sulfuric acid at 25 °C was used as the solvent due to security and health issues with a polymer concentration of 0,005 g/cm³.

Part and mechanical properties

The part thickness and width were measured by a micrometer at three positions. The density was calculated by the part volume and weight. A precision scale was used to determine the part weight. The surface roughness was measured using a tactile stylus instrument Waveline 20, with a stylus tip of 2 µm and an attaching force of 0.8 mN. The roughness R_a was determined according to [19]. The specimens were conditioned in a vacuum after removing from the part cake leading to a dry state. The mechanical properties were measured following [20] with a speed of 0.5 mm/min for the Young's modulus and 2.5 mm/min for the elongation at break with a testing machine of the type 1484 from Zwick Roell.

Results and Discussion

For a detailed understanding of the aging effects occurring and the stability of the manufactured powders, time-dependent data is essential. Within the PBF-LB/P process, it is impossible to generate powder samples with a defined thermal history, atmospheric conditions, and aging time. Therefore, experiments with well-defined boundary conditions are conducted. Structural changes in the polymer chain can influence the melt rheology, with chain scission leading to a decrease in viscosity and chain elongation increasing viscosity. The frequency-dependent rheological behavior is to demonstrate structural changes in the polymer. The viscosity of the reference material (Figure 1, left) shows no change up to 109 minutes. After this time, the viscosity increases at low frequencies, progressively increasing with time. This increase can indicate cross-linking. D1 (Figure 1, middle) exhibits good aging stability with little to no change over the measured time. D2 (Figure 1, right) exhibits a similar increase in viscosity at low frequencies, starting at 109 minutes. Overall, both D1 and D2 illustrate an increased viscosity compared to the reference, suggesting that the antioxidants are working already in the powder manufacturing process. Furthermore, the reference material shows an increase in viscosity for all measurements at frequencies lower than 2 rad/s, indicating aging effects occurring in the powder manufacturing process.

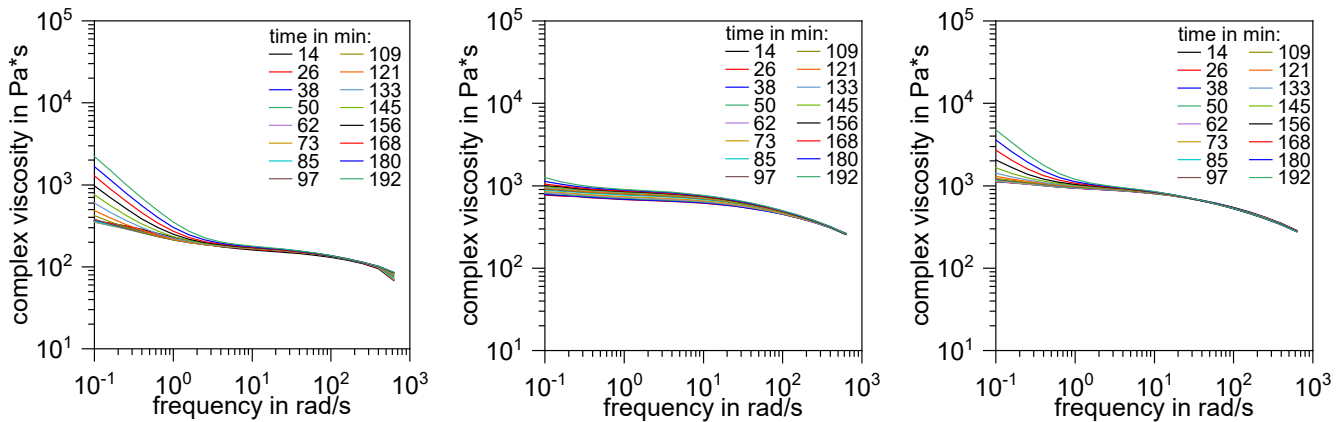


Figure 1: Rheological aging behavior under defined boundary conditions, Ref. (left), D1 (middle), D2 (right), T = 230 °C, air atmosphere

The FTIR analyses provide a deeper understanding of occurring aging mechanisms. Figure 2 (left) displays the full spectrum of the FTIR for the reference material, with each line representing a spectrum taken at a 1-minute delay. Important peaks are marked to enhance understanding. For oxidation, the range between 1700 and 1800 cm^{-1} (Figure 2, middle) is of particular significance, where changes associated with degradation products resulting from oxidation are observed. Examples of such changes include the presence of carboxyl or ester groups. In the reference material, the formation of these peaks is observed over time. Figure 2 (right) shows the peak changes (1716 cm^{-1} , ketone) for the reference material, D1, and D2. While the reference material shows an immediate increase, D1, and D2 exhibit stable peaks for up to 30 minutes. After 30 minutes, the peak of D2 starts to increase, while D1 remains stable up to 60 minutes. This indicates the stabilizing effect of the used antioxidants.

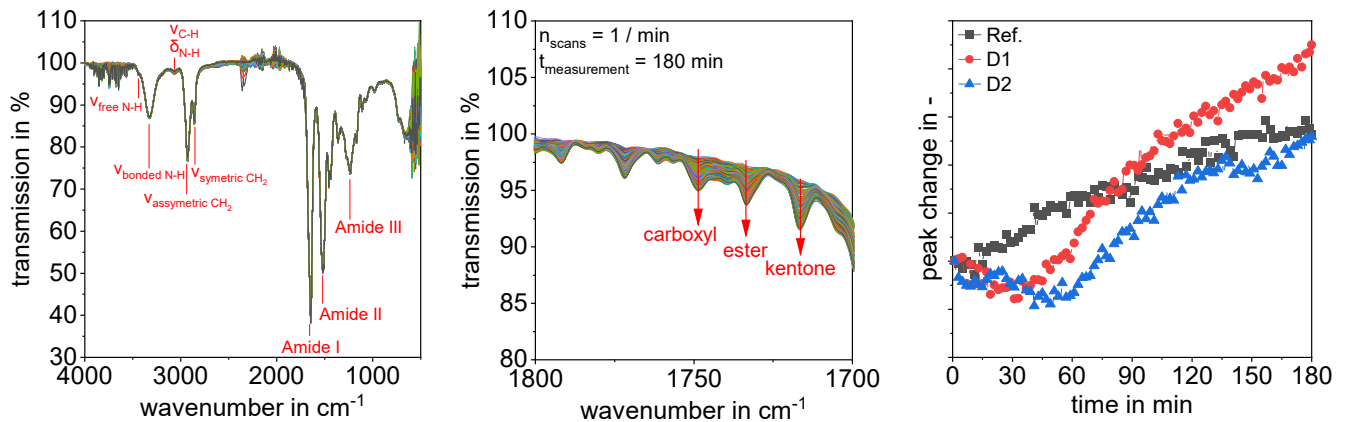


Figure 2: Full spectrum of the FTIR-Measurement for the reference material (left), Carboxyl groups for the reference material (middle) and peak change at 1716 cm^{-1} for all three materials (right)

For processing, the particle size distribution (PSD) of the powder plays a crucial role in powder bed fusion of polymers, as it directly impacts the density of the powder bed and the recoating behavior. The measurements conducted in this study indicate that the additives used did not have a significant influence on these factors (Figure 3, left). The $d_{50.3}$ is approximately 80 μm , with a slightly increased fraction of smaller particles. The largest particles observed are up to 200 μm . The PSD is considered suitable for the process. SEM analysis reveals the presence of typical edgy particles, which are commonly observed in cryogenic milling processes (Figure 3, middle). Edgy particles can lead to bad recoating behavior. The powders without any additives are shown to exhibit a rough and cracked powder bed (Figure 3, right). However, the use of flow agents can enhance powder flowability, resulting in a smoother powder bed. The addition of hydrophobic silica increases the distance between particles and reduces adhesion forces, promoting better particle flow. Pyrogenic alumina acts as an antistatic agent, preventing the buildup of static charges. Overall, the size distribution of the powder, the particle shape, and the use of flow agents and antistatic agents play critical roles in determining the quality and behavior of the powder bed in polymer powder bed fusion processes. The additives used show no influence on these values.

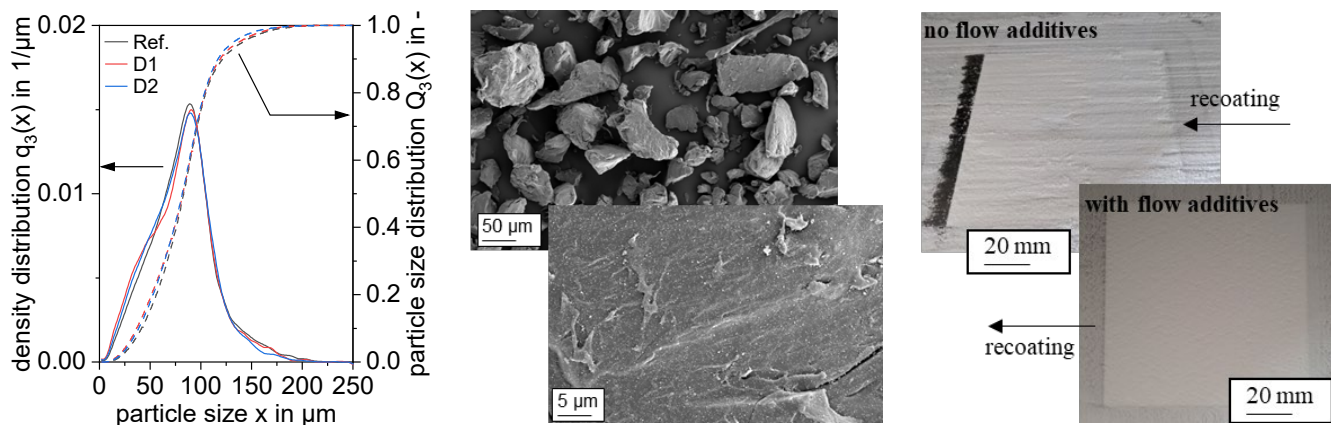


Figure 3: Particle size distribution w/o flow additives (left), particle shape, and detailed SEM images of the particle surface (middle), powder recoating behavior (left)

Additionally added additives can influence the thermal behavior of a polymer, therefore impacting the processing window of a PBF-LB/P powder. Figure 4 (left) shows the dynamic DSC-measurements of the three powder materials. For the melting peak of the first heating, no significant difference is detected. For the first cooling, a slight shift of the crystallization peak to lower temperatures is observed for D1 and D2 compared to the reference powder. This indicates that the used antioxidants have no nucleating effect. The measured processing windows for all three materials are shown in Figure 4 (middle) with a slightly wider processing window for D1 and D2. While the dynamic DSC is an indicator of the processing temperature and the processing window, it is hard to transfer the results to the PBF-LB/P process. In process, the thermal boundary conditions differ strongly from the 10 K/min heating and cooling rate. Therefore, Figure 4 (right) displays isothermal measurements for the virgin powders. Compared to the reference, the crystallization peak of the D1 and D2 powder is shifted to shorter times, indicating a nucleation effect. These results indicate that process adapted measurements like isothermal DSC-measurements are important to understand the material behavior in the process. A shorter isothermal crystallization time can lead to warpage or process termination due to curling.

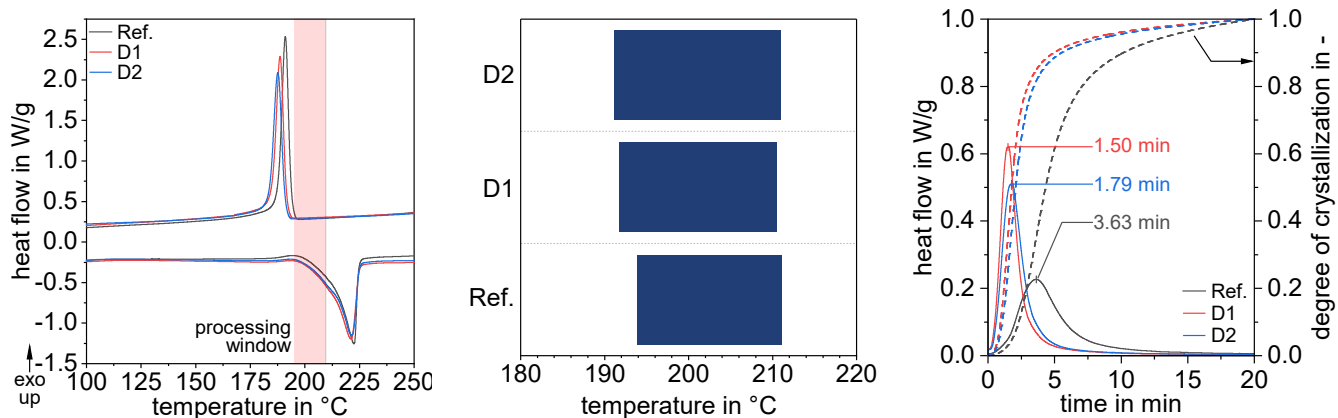


Figure 4: Dynamic DSC-Measurements of the three materials (left), measured processing window (middle), and isothermal Measurements of the virgin powder, $T_{iso} = 200\text{ °C}$ (right)

Due to thermo-mechanical stress in the recoating process, the powder flowability is reduced over the process. This physical aging mechanism can lead to smoothing of the particle surface or flow additives which are pressed into the material. Both lead to a decrease of the particle – particle distance and leads to a decreased powder flowability. Figure 5 (left) shows the measured compression depths for the three powders in virgin state and after one processing cycle. In the virgin state, the powders indicate a similar compression depth. After processing, a slight increase for the D1 and D2 powder is measured compared to the reference material. This may lead to problems in recoating or a decrease of the powder bed density. Overall, D1 and D2 show only a small increase which should not affect the process significantly.

To analyze the chemical aging, the viscosity number (VN) of the virgin and used powder is measured (Figure 5, middle). The reference powder in the virgin state shows an already decreased VN compared to D1 and D2. The same behavior was analyzed in the rheological measurements of the viscosity (Figure 1Figure 5). This suggests a stabilising effect of the used antioxidants in the powder manufacturing process. After processing, the VN decreases strongly for all materials. This indicates chain scissoring due to thermal oxidation. Due to the reactive end groups, polyamides tend to increase in molecular weight (post-condensation). Figure 5 (right) details the change of the VN. D2 shows the smallest change, which indicates that the antioxidants used are more suitable compared to D1.

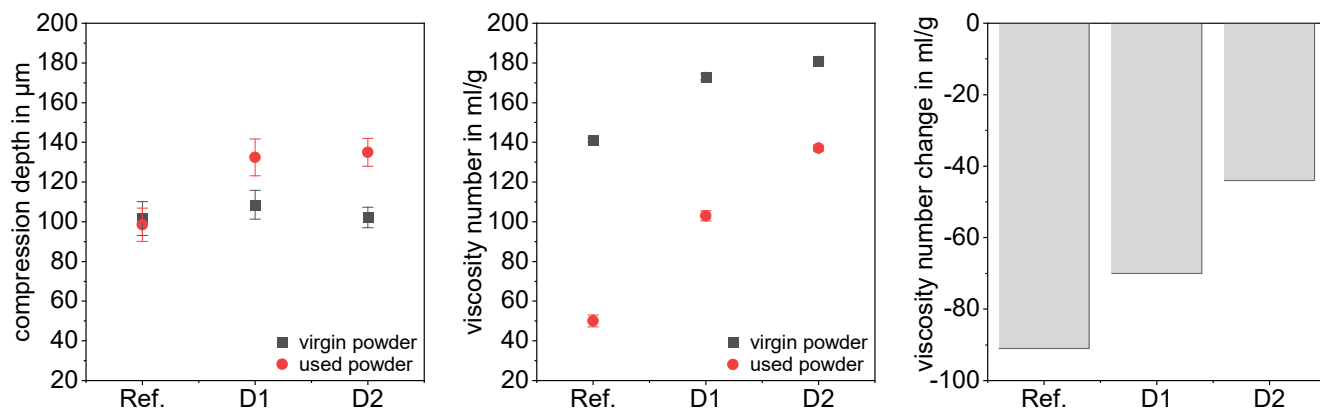


Figure 5: Compression depth measurements of the virgin and used powder (left), viscosity number (middle), and change of the viscosity number due to aging (right)

While material aging plays a crucial role in reuse, processing, and part properties, thermo-oxidation can cause discoloration of the polymer. Although this change does not directly correlate with the part properties, a discolored part cannot be sold. Figure 6 (left) displays the virgin powder, used powder, and the produced part. Slight discoloration is observed for D1 and the reference material compared to D2 in the virgin powder; this indicates the stabilizing effect during the powder manufacturing process. After one cycle, both the powder and parts exhibit significant discoloration for all three materials. The reference material shows the strongest color

change, severely limiting the reuse of the powder, especially for larger build jobs where this effect is expected to amplify. Figure 6 (right) presents the measured yellowness index, where the reference material exhibits the most pronounced changes. Overall, the use of antioxidants demonstrates a reduction in the discoloration of polyamide 6.

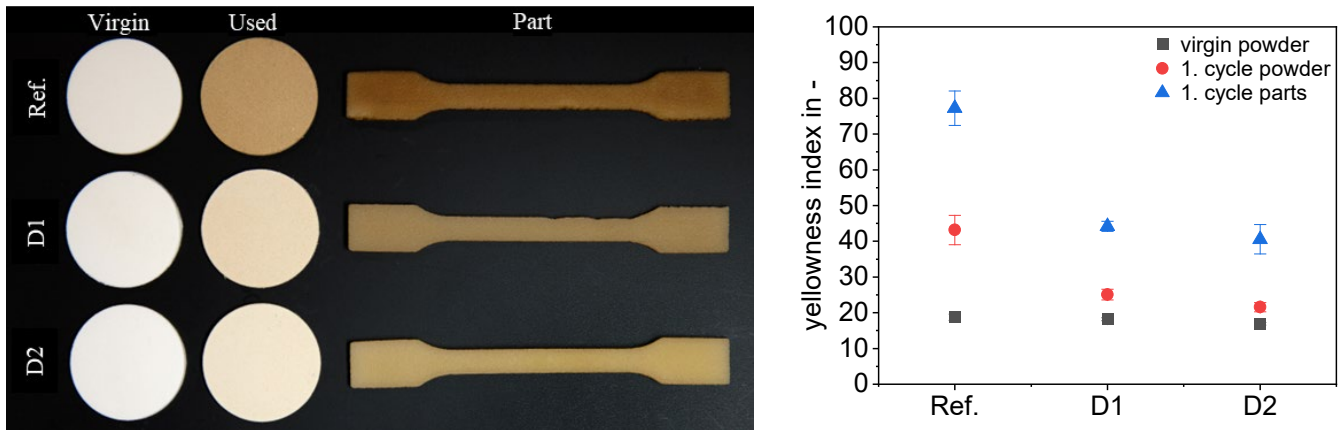


Figure 6: Discoloration of the virgin powder, used powder and parts (left), yellowness index (right)

Figure 7 displays thin cuts of the manufactured parts obtained from the center of the tensile bars. The reference material (Figure 7, left) exhibits poor geometrical accuracy and a high number of round pores within the part. These pores may indicate polymer degradation during processing. In comparison, D1 (Figure 7, middle) and D2 (Figure 7, right) show no pores, good layer bonding, minimal presence of non-molten particles, and well-defined geometrical shapes. The inferior geometry of the reference material can be attributed to its decreased viscosity and VN.

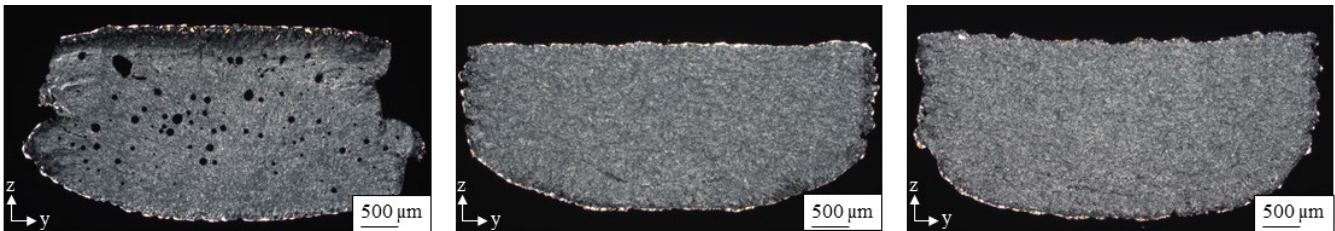


Figure 7: Thin cuts obtained from the center of the manufactured tensile bars, reference material (left), D1 (middle), D2 (right)

The presence of the shown pores leads to a decrease in part density for the reference material (Figure 8, left). The density increases for D1 and reaches its highest value for D2. While the thin cuts only indicate the local position of the tensile bar, the density considers the entire bar. Pores located in the shoulder or other positions of the tensile bar can reduce the part density, suggesting that D2 exhibits the highest density and the lowest pore volume. In addition to density, the surface roughness of the part plays a critical role in its mechanical properties. D2 exhibits a slightly increased surface roughness compared to the reference material and D1. The surface roughness is primarily influenced by the particle system used and the presence of partially molten particles on the surface area.

The measured E-Modulus shows an increase for the D1 and D2 materials compared to the reference material (Figure 8, middle). Material properties can be influenced by aging effects, which in turn affect the E-Modulus. Additionally, the geometry and presence of pores can result in an inaccurate measurement of the cross-section, further contributing to the lower E-Modulus observed in the reference material. Regarding elongation at break, a significant increase is observed for D1 and D2 compared to the reference material (Figure 8, right). The elongation at break is a sensitive parameter for aging mechanisms in PBF-LB/P suggesting that antioxidants can improve the mechanical properties of the manufactured parts while also reducing thermo-oxidation of the material.

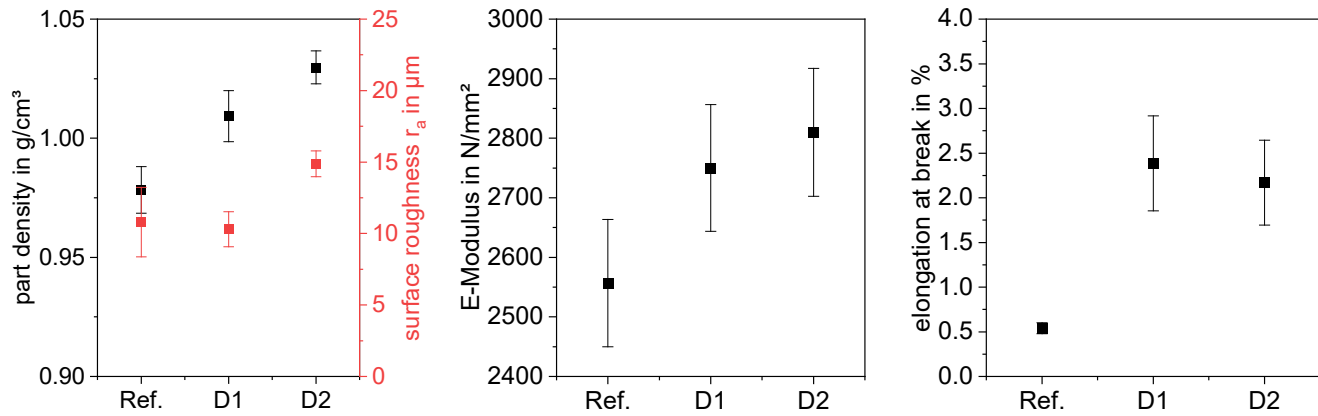


Figure 8: Part density and surface roughness of the tensile bars (left, measured e-modulus (middle) and elongation at break (right))

Summary and Outlook

This scientific paper presents a comprehensive study of the effects of aging on the properties of polyamide 6 powders used in PBF-LB/P processes. The experiments conducted in the study include particle size distribution, compression depth, DSC measurements, rheology and FTIR, viscosity number, and part and mechanical properties.

The study used a combined measurement instrument called the rheonaut to measure the time-dependent aging effects under defined boundary conditions. The results revealed that the viscosity of the reference material showed no change up to 109 minutes, after which it increased at low frequencies, indicating cross-linking due to aging effects. The FTIR measurements provided a deeper understanding of the aging mechanisms at play. The results showed that the reference material exhibited an immediate increase in the formation of peaks associated with degradation products resulting from oxidation, such as the presence of carboxyl or ester groups. However, D1 and D2 exhibited stable peaks for up to 30 and 60 minutes, respectively, indicating the stabilizing effect of the used antioxidants.

The particle size distribution was determined using image analysis, and the results indicated that the additives used did not significantly PSD or the recoating behavior. All grinded powder materials needed additional flow additives for a suitable recoating behavior. The compression depth was measured using a rotational rheometer, and the results showed a slight increase in compression depth for D1 and D2 powders after processing, which could potentially lead to recoating problems or a decrease in powder bed density. Further, dynamic and isothermal measurements were performed to characterize the melting and crystallization behavior of the powders. The results showed that the used antioxidants did have a nucleating effect for the isothermal crystallization. The dynamic measurements showed slightly wider processing window for D1 and D2.

The viscosity number was determined to characterize the changes in viscosity and average molecular weight due to aging in the process. The results showed that the viscosity number decreased strongly for all materials after processing, indicating chain scissoring due to thermal oxidation. D2 showed the smallest change and, therefore, the best aging stability for the used powders.

The study also examined the discoloration of the polymer due to thermo-oxidation, which, while not directly affecting the part properties, can impact the marketability of the product. The results showed that slight discoloration could be observed for D1 and the reference material compared to D2 in the virgin powder, indicating the stabilizing effect during the powder manufacturing process. After one cycle, both the powder and parts exhibited significant discoloration for all three materials. The reference material showed the strongest color change, severely limiting the reuse of the powder, especially for larger build jobs where this effect is expected to amplify. However, the use of antioxidants demonstrated a reduction in the discoloration of polyamide 6. The yellowness index measurements confirmed these observations, with the reference material exhibiting the most pronounced changes.

The manufactured tensile bars show that D2 exhibited the highest density and the lowest pore volume. Further, the mechanical properties were measured, and the results showed an increase in the E-Modulus for D1 and D2 materials compared to the reference material. Additionally, a significant increase in elongation at break was

observed for D1 and D2 compared to the reference material. In conclusion, the study found that the use of antioxidants can improve the mechanical properties of the manufactured parts while also reducing thermo-oxidation of the material.

Acknowledgment

This study is funded within the IGF project (21598 N) with the title "Improving the aging stability of plastic powders for selective laser sintering by tailor-made additive systems". The authors would like to thank Niels Brauch of the Fraunhofer Institute for Operational Stability and System Reliability (LBF) in Darmstadt for material selection and compounding. In addition, the authors would like to thank Florentin Tischer of the Institute of Particle Technology at the FAU Erlangen-Nürnberg for providing particle size distribution data.

References

- [1] M. Schmid, Laser sintering with plastics: technology, processes, and materials, First edition, Hanser Publishers ; Hanser Publications, Cincinnati : Munich, 2018.
- [2] Wohlers Associates, ed., Wohlers report 2022: 3D printing and additive manufacturing global state of the industry, Wohlers Associates, Fort Collins (Colo.), 2022.
- [3] G.W. Ehrenstein, S. Pongratz, Beständigkeit von Kunststoffen. Bd. 2: ..., Hanser, München, 2007.
- [4] B. Doležel, C.-M. von Meysenbug, Die Beständigkeit von Kunststoffen und Gummi, 1. Aufl, Hanser, München, 1978.
- [5] K. Wudy, D. Drummer, Aging effects of polyamide 12 in selective laser sintering: Molecular weight distribution and thermal properties, Additive Manufacturing. 25 (2019) 1–9. <https://doi.org/10.1016/j.addma.2018.11.007>.
- [6] K. Wudy, Alterungsverhalten von Polyamid12 beim selektiven Lasersintern, Lehrstuhl für Kunststofftechnik, Erlangen, 2017.
- [7] C.D. Papaspyrides, S.N. Vouyiouka, eds., Solid state polymerization, Wiley, Hoboken, N.J, 2009.
- [8] H. Zarringhalam, N. Hopkinson, N.F. Kamperman, J.J. de Vlieger, Effects of processing on microstructure and properties of SLS Nylon 12, Materials Science and Engineering A. 435–436 (2006) 172–180. <https://doi.org/10.1016/j.msea.2006.07.084>.
- [9] C. Mielicki, A. Wegner, B. Gronhoff, J. Wortberg, G. Witt, Prediction of PA12 melt viscosity in laser sintering by a time and temperature dependent rheological model, RTejournal. 32 (2012).
- [10] C. Mielicki, Prozessnahes Qualitätsmanagement beim Lasersintern von Polyamid 12, PhD Thesis, 2014. <https://duepublico.uni-due.de/servlets/DocumentServlet?id=36152>.
- [11] O. Okamba-Diogo, E. Richaud, J. Verdu, F. Fernagut, J. Guilment, B. Fayolle, Investigation of polyamide 11 embrittlement during oxidative degradation, Polymer. 82 (2016) 49–56. <https://doi.org/10.1016/j.polymer.2015.11.025>.
- [12] B. Fayolle, L. Audouin, J. Verdu, A critical molar mass separating the ductile and brittle regimes as revealed by thermal oxidation in polypropylene, Polymer. 45 (2004) 4323–4330. <https://doi.org/10.1016/j.polymer.2004.03.069>.
- [13] C.H. Do, E.M. Pearce, B.J. Bulkin, H.K. Reimschuessel, FT–IR spectroscopic study on the thermal and thermal oxidative degradation of nylons, J. Polym. Sci. A Polym. Chem. 25 (1987) 2409–2424. <https://doi.org/10.1002/pola.1987.080250908>.
- [14] J. Pospíšil, Mechanistic action of phenolic antioxidants in polymers—A review, Polymer Degradation and Stability. 20 (1988) 181–202. [https://doi.org/10.1016/0141-3910\(88\)90069-9](https://doi.org/10.1016/0141-3910(88)90069-9).
- [15] K. Schwetlick, W.D. Habicher, Organophosphorus antioxidants action mechanisms and new trends, Angew. Makromol. Chemie. 232 (1995) 239–246. <https://doi.org/10.1002/apmc.1995.052320115>.
- [16] DIN EN ISO 527-2: 2012-06, Beuth Verlag GmbH
- [17] S. Cholewa, A. Jaksch, D. Drummer, Structure Development of Semi-crystalline Polymers in Laser Based Powder Bed Fusion, in: Antec 2023, 2023.
- [18] S. Greiner, A. Jaksch, S. Cholewa, D. Drummer, Development of material-adapted processing strategies for laser sintering of polyamide 12, Advanced Industrial and Engineering Polymer Research. (2021) S2542504821000294. <https://doi.org/10.1016/j.aiepr.2021.05.002>.
- [19] DIN EN ISO 4287:2010-07, Beuth Verlag GmbH
- [20] DIN EN ISO 527-1: 2019-12, Beuth Verlag GmbH